Spectroscopic Studies and Electronic Structure Description of the High Potential Type 1 Copper Site in Fungal Laccase: Insight into the Effect of the Axial Ligand

Amy E. Palmer,[†] David W. Randall,[†] Feng Xu,*[,‡] and Edward I. Solomon*[,†]

Contribution from the Department of Chemistry, Stanford University, Stanford, California 94306, and Novo Nordisk Biotechnology, Davis, California 95616

Received April 5, 1999. Revised Manuscript Received June 9, 1999

Abstract: A variety of spectroscopic techniques combined with density functional calculations are used to describe the electronic structure of the nonaxially ligated, trigonal planar type 1 copper site in three fungal laccases with substantially different type 1 copper reduction potentials. These methods are also applied to a mutant of the high-potential *Polyporus pinsitis* laccase in which the nonligating axial phenylalanine (Phe) is changed to methionine (Met). Optical absorption, circular dichroism, and magnetic circular dichroism spectroscopies of all three fungal laccases reveal that, relative to the classic blue copper protein plastocyanin, the ligand field strength at the type 1 Cu center and the oscillator strength of the charge-transfer transitions increase. Resonance Raman spectra show that the envelope of Cu−S(Cys) stretching bands is shifted to higher energy in the fungal laccases, implying a stronger Cu−S(Cys) bond. Differences in the EPR spectra of the fungal laccases and plastocyanin are found to result from the increased ligand field and decreased 4s mixing into the Cu $d_{x^2-y^2}$ half-filled, highest occupied molecular orbital (HOMO). All three fungal laccases display similar spectroscopic properties despite their differing reduction potentials. Electronic absorption, circular dichroism (CD), magnetic circular dichroism (MCD), resonance Raman, and EPR spectroscopies show significant perturbation of the electronic structure of the fungal laccase type 1 copper site upon mutation of the axial Phe to Met, consistent with the site becoming more like that in plastocyanin, which has an axial Met ligand; the ligand field decreases, covalency of the Cu−S(Cys) bond decreases, and the Raman shifts of the Cu−S stretching bands decrease. Density functional calculations on the fungal laccase site provide insight into the origin of the experimentally observed increase in covalency and ligand field strength. These calculations show that it is the elimination of the Met ligand donor interaction that leads to an increase in the donor strength of the S(Cys). The contribution of the axial ligand to the reduction potential is discussed.

Introduction

Laccase (*p*-diphenol: dioxygen oxidoreductase, EC 1.10.3.2) belongs to the family of multicopper oxidases that includes ascorbate oxidase, ceruloplasmin, and FET3.[1,2] Functionally, all multicopper oxidases couple four one-electron substrate oxidations with the four-electron reduction of dioxygen to water. Spectroscopic studies, sequence alignments, and crystal structure comparisons reveal that all multicopper oxidases contain at least one type 1 (T1), one type 2 (T2), and one type 3 (T3) Cu center.[1−4] These different Cu sites are defined by the spectroscopic properties they exhibit in the oxidized (Cu^{2+}) state. The T1, or blue, Cu site is distinguished by an intense ($\epsilon \approx 5000$ M^{-1} cm^{-1}) absorption (abs) feature around 600 nm and small ($<100 \times 10^{-4}$ cm^{-1}) parallel hyperfine coupling in electron paramagnetic resonance (EPR). The T2, or normal, Cu site displays parallel hyperfine coupling ($>160 \times 10^{-4}$ cm^{-1}) typical of normal tetragonal Cu and does not exhibit intense features in the visible absorption or CD spectrum. The T3, or coupled binuclear, Cu site is comprised of two Cu^{2+} ions that are antiferromagnetically coupled through a bridging hydroxide.[5] The resulting diamagnetic ($S_{total} = 0$) T3 Cu site lacks an EPR signal, but it displays an absorption feature around 330 nm ($\epsilon \approx 5000$ M^{-1} cm^{-1}). Laccase is the simplest of the multicopper oxidases, containing one of each type of Cu for a total of four Cu atoms. Ascorbate oxidase (AO) is essentially a dimer of laccase-like subunits while ceruloplasmin (CEP) is more complex.[5,6] The AO[5] and CEP[6] crystal structures confirm spectroscopic results[7,8] showing that the T2 and T3 Cu sites are in close proximity (within 4 Å) and together form a trinuclear Cu cluster. Similarly, although the crystal structure of fungal laccase is of a T2 depleted form of the enzyme, it indicates that an analogous trinuclear Cu cluster exists in the native enzyme.[9] The T1 Cu site in fungal laccase accepts electrons from the substrate, typically diphenols, aryl diamines, or amino

[†] Stanford University.
[‡] Novo Nordisk Biotechnology.

(1) Solomon, E. I.; Sundaram, U. M.; Machonkin, T. E. *Chem. Rev.* **1996**, *96*, 2563−2605.
(2) Messerschmidt, A. *Multi-copper Oxidases*; Messerschmidt, A., Ed.; World Scientific: River Edge, NJ, 1997.
(3) Messerschmidt, A.; Huber, R. *Eur. J. Biochem.* **1990**, *187*, 341−352.
(4) Dooley, D. M.; Rawlings, J.; Dawson, J. H.; Stephens, P. J.; Andréasson, L.-E.; Malmström, B. G.; Gray, H. B. *J. Am. Chem. Soc.* **1979**, *101*, 5038−5046.
(5) Messerschmidt, A.; Ladenstein, R.; Huber, R.; Bolognesi, M.; Avigliano, L.; Petruzzelli, R.; Rossi, A.; Finazzi-Agró, A. *J. Mol. Biol.* **1992**, *224*, 179−205.
(6) Zaitseva, I.; Zaitsev, V.; Card, G.; Moshov, K.; Bax, B.; Ralph, A.; Lindley, P. *J. Biol. Inorg. Chem.* **1996**, *1*, 15−23.
(7) Spira-Solomon, D. J.; Allendorf, M. D.; Solomon, E. I. *J. Am. Chem. Soc.* **1986**, *108*, 5318−5328.
(8) Cole, J. L.; Tan, G. O.; Yang, E. K.; Hodgson, K. O.; Solomon, E. I. *J. Am. Chem. Soc.* **1990**, *112*, 2243−2249.

10.1021/ja991087v CCC: $18.00
Published on Web 07/21/1999

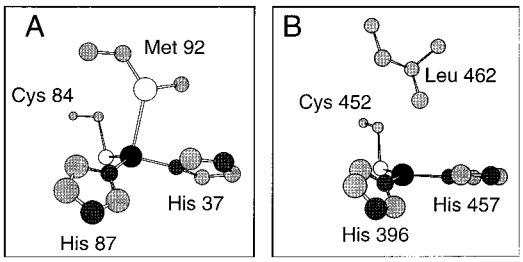

Figure 1. Comparison of the T1 Cu site in plastocyanin[10] (A) with *Coprinus cinereus* fungal laccase[9] (B).

phenols, and then transfers the electrons over 13 Å to the T2/T3 trinuclear Cu cluster where dioxygen is reduced to H_2O.[1]

A plethora of comparative studies have established that the copper coordination of the T2 and T3 centers is very similar among the multicopper oxidases; however, there are differences in the T1 Cu ligation. The classic T1 Cu coordination environment, such as that found in plastocyanin (Figure 1A), involves a short Cu−S from Cys (∼2.1 Å), a long Cu−S from Met (∼2.8 Å), and two fairly typical Cu−N from His (∼2.0 Å).[10] This ligation pattern is also observed for the T1 Cu in ascorbate oxidase, two of the three T1 coppers of human ceruloplasmin, and the tree laccases. In contrast, sequence alignments suggest that laccases isolated from fungi possess a leucine (Leu) or phenylalanine (Phe) rather than a methionine at the axial position.[1,3,11] These amino acids do not contain functional groups that can ligate to the Cu and are too bulky to allow water to bind. The recent crystal structure of *Coprinus cinereus* laccase confirms that the T1 Cu in this fungal laccase forms a trigonal planar site with two N_{His} and one S_{Cys} ligands and, most importantly, no axial ligand (Figure 1B).[9]

The nature of the blue copper site has been the subject of extensive studies that relate the unique electronic structure of this site with its function as an electron-transfer center.[12−14] A combination of experimental and theoretical studies have elucidated a number of important properties of the blue Cu site. There is very little geometry change upon reduction from Cu^{2+} to Cu^{1+}, indicating that the site has a low reorganization energy associated with electron transfer.[15,16] The Cu−S_{Cys} bond is highly covalent,[17−19] providing an efficient hole superexchange pathway for electron transfer through this residue.[20] The strength of the Cu−S_{Cys} bond appears to be inversely related to the strength of the axial Cu−S_{Met} interaction (the weaker the Met, the stronger the Cys).[21] The reduction potential of the oxidized T1 Cu site tends to be higher than that of aqueous Cu^{2+}.[22] Further insight into the origin of these properties may be gained by looking at systematic differences in the experimental data and electronic structures of a series of blue copper proteins with axial interactions of varying strength. The electronic structures of the classic T1 site in plastocyanin as well as a number of perturbed T1 sites (nitrite reductase, cucumber basic blue, and stellacyanin) have now been examined.[19,21,23,24] The perturbed sites fall into two classes: those exhibiting a tetragonal distortion with increasing axial interaction (pseudoazurin, cucumber basic protein, and nitrite reductase) and those displaying a tetrahedral distortion (stellacyanin).[21] In both cases the change in electronic structure in the perturbed centers was linked to the axial ligand interaction. The blue copper site in fungal laccase is of particular interest in relation to other blue copper proteins because it lacks an axial ligand.

Table 1. Comparison of Redox Potentials of the T1 Cu

enzyme	$E°$ [a]	axial
Myceliophtora thermophila laccase	450−480[b]	Leu
Rhizoctonia solani laccase	630−680[b]	Leu
Polyporus pinsitus Laccase	750−790[b]	Phe
Polyporus pinsitus laccase F463M	680[c]	Met
spinach plastocyanin	370[d]	Met

[a] Units of mV vs NHE. [b] From ref 26. [c] From ref 30. [d] From ref 21.

In this study, we examine the T1 Cu in three different fungal laccases where the axial ligand is absent, *Myceliophthora thermophila* (M.t.), *Rhizoctonia solani* (R.s.), and *Polyporus pinsitis* (P.p.).[25] From sequence comparisons and EPR data,[26] these enzymes appear to have identical T1 Cu ligation, and yet they exhibit a range (500−800 mV) of redox potentials (Table 1). In this study, we use absorption, circular dichroism (CD), magnetic circular dichroism (MCD), EPR, and resonance Raman spectroscopies to elucidate the spectral features of these enzymes. Parallel studies of fluoride derivatives are used to differentiate the spectral features of the T1 from those of the trinuclear Cu cluster. The spectroscopic results are combined with density functional calculations to gain insight into the electronic structure of this unique, nonaxially ligated, trigonal planar T1 Cu site. In addition, we examine a mutant in which the axial Phe of the high potential *Polyporus pinsitis* laccase was mutated to a Met to gain further insight into the contribution of the axial Met ligand to the electronic structure. Finally, the electronic structure of these enzymes is compared to that of the classic blue copper site in plastocyanin and the origins of their spectral and redox differences are discussed.

Experimental Section

Enzyme Characterization. *Myceliophtora thermophila* laccase, *Rhizoctonia solani* laccase, *Polyporus pinsitis* laccase, and the axial F463M mutant of *Polyporus pinsitis* laccase were cloned and expressed

(9) Ducros, V.; Brzozowski, A. M.; Wilson, K. S.; Brown, S. H.; Østergaard, P.; Schneider, P.; Yaver, D. S.; Pedersen, A. H.; Davies, G. J. *Nat. Struct. Biol.* **1998**, *5*, 310−316.
(10) Guss, J. M.; Bartunik, H. D.; Freeman, H. C. *Acta Crystallogr.* **1992**, *B48*, 790−811.
(11) Germann, U. A.; Müller, G.; Hunziker, P. E.; Lerch, K. *J. Biol. Chem.* **1988**, *263*, 885−896.
(12) Solomon, E. I.; Baldwin, M. J.; Lowery, M. D. *Chem. Rev.* **1992**, *92*, 521−542.
(13) Solomon, E. I.; Lowery, M. D. *Science* **1993**, *259*, 1575−1581.
(14) Adman, E. T. In *Advances in Protein Chemistry*; Anfinsen, C. B., Richards, F. M., Edsall, J. T., Eisenberg, D. S., Ed.; Academic Press: San Diego, 1991; pp 145−197.
(15) Guss, J. M.; Harrowell, P. R.; Murata, M.; Norris, V. A.; Freeman, H. C. *J. Mol. Biol.* **1986**, *192*, 361−387.
(16) Guckert, J. A.; Lowery, M. D.; Solomon, E. I. *J. Am. Chem. Soc.* **1995**, *117*, 2817−2844.
(17) Shadle, S. E.; Penner-Hahn, J. E.; Schugar, H. J.; Hedman, B.; Hodgson, K. O.; Solomon, E. I. *J. Am. Chem. Soc.* **1993**, *115*, 767−776.
(18) George, S. J.; Lowery, M. D.; Solomon, E. I.; Cramer, S. D. *J. Am. Chem. Soc.* **1993**, *115*, 2698−2969.
(19) Gewirth, A. A.; Solomon, E. I. *J. Am. Chem. Soc.* **1988**, *110*, 3811−3819.
(20) Lowery, M. D.; Guckert, J. A.; Gebhard, M. S.; Solomon, E. I. *J. Am. Chem. Soc.* **1993**, *115*, 3012−3013.
(21) LaCroix, L. B.; Randall, D. W.; Nersissian, A. M.; Hoitink, C. W. G.; Canters, G. W.; Valentine, J. S.; Solomon, E. I. *J. Am. Chem. Soc.* **1998**, *120*, 9621−9631.
(22) Sykes, A. G. In *Advances in Inorganic Chemistry*; Academic Press: New York, 1991; Vol. 36, pp 377−408.
(23) LaCroix, L. B.; Shadle, S. E.; Wang, Y.; Averill, B. A.; Hedman, B.; Hodgson, K. O.; Solomon, E. I. *J. Am. Chem. Soc.* **1996**, *118*, 7755−7768.
(24) By perturbed we mean an increase in absorption at 450 nm and a rhombic EPR spectrum.
(25) This enzyme has a high degree of homology with *Polyporus versicolor* laccase. It should be noted that *Polyporus pinsitis* is also referred to as *Trametes villosa*, and *Polyporus versicolor* is often referred to as *Trametes versicolor*.
(26) Xu, F.; Shin, W.; Brown, S. H.; Wahleithner, J. A.; Sundaram, U. M.; Solomon, E. I. *Biochim. Biophys. Acta* **1996**, *1292*, 303−311.

as described previously.[27−30] Enzyme concentrations were determined using the absorption band at 280 nm ($\epsilon_{280} = 146$ mM^{-1} cm^{-1} for M.t.L, 66 mM^{-1} cm^{-1} for R.s.L, and 80 mM^{-1} cm^{-1} for P.p.L and P.p.L F463M). Copper concentrations were determined spectrophotometrically using 2,2′-biquinoline[31] or by atomic absorption spectroscopy. The concentration of paramagnetic copper was determined from spin quantitation of EPR spectra (vide infra). Spectra were normalized to copper concentration. All experiments were performed in 100 mM potassium phosphate buffer, pH = 6 (pD = 5.6 for MCD experiments). Chemicals used as buffers were reagent grade and were used without further purification. Water was purified to a resistivity of 15−18 MΩ using a Barnstead Nanopure deionizing system.

Isolation of the T1 Cu. Fluoride adduct samples were prepared by incubating eqimolar amounts of NaF and protein for 24 h at 4 °C. Samples were then characterized by absorption, CD, and MCD. To selectively reduce the T1 Cu (vide infra), F^- adduct samples were treated anaerobically with 1−5 electron equiv of sodium ascorbate. Samples were then transferred anaerobically to quartz EPR tubes, MCD cells, or optical quartz cuvettes for further spectroscopic characterization. Glassed samples for MCD were prepared in deuterated buffer and 50% (v/v) D_2O/glycerol-d_3. Addition of glycerol had no effect on the CD spectrum of the proteins.

Spectroscopic Studies. Room-temperature UV/visible absorption spectra were obtained using a Hewlett-Packard HP8452A diode array spectrophotometer in 1.0, 0.2, or 0.1 cm quartz cuvettes. Room-temperature CD and low-temperature (5 K) MCD spectra in the 300−800 nm region were collected with a Jasco J-500-C spectropolarimeter operating with an S-20 photomultiplier tube and an Oxford SM4-7T magnet. CD and MCD spectra in the 700−2000 nm region were recorded with a Jasco J-200-D spectropolarimeter, a liquid nitrogen cooled InSb detector, and an Oxford SM4000-7T magnet. CD samples were run in a 1.0 cm quartz cuvette. MCD samples were run in MCD cells fitted with quartz disks and a 0.3 cm rubber gasket spacer. Depolarization of light by the MCD samples was monitored by the effect it had on the CD spectrum of nickel (+)-tartrate placed before and after the sample. Depolarization was less than 5%. Simultaneous Gaussian fitting of the absorption, CD, and MCD spectra was performed using the PeakFit program (Jandel). EPR spectra were obtained using a Bruker ER 220D-SRC spectrometer. All samples were run at 77 K in a liquid nitrogen finger Dewar. Spin quantitation of the EPR spectra was accomplished using a Cu standard, $Cu(ClO_4)_2$,[32] of known concentration run in the same tube as the sample. Simulations of EPR spectra were performed using the program SIM15 obtained from the Quantum Chemistry Program Exchange. Resonance Raman spectra were collected with a Princeton Instruments ST-135 back-illuminated CCD detector on a Spex 1877 CP triple monochromator with 1200, 1800, and 2400 grooves/mm holographic spectrograph gratings. A Coherent I90C Kr^+ ion laser provided excitation at 647.1 nm. A polarization scrambler was used between the sample and the spectrometer. The Raman scattering energy was calibrated with CH_3CH_2CN. Frequencies are accurate to within <2 cm^{-1}. Samples tubes were spun by an air-driven NMR tube spinner and were run at ∼180 K, with the temperature maintained by a N_2 flow system. The intensity-weighted average $\langle \nu_{Cu-S} \rangle$ of the complex Cu−S stretching envelope was calculated using $[\sum I_{01}\nu^2]/[\sum I_{01}\nu]$, where I_{01} is the resonance Raman intensity of a particular mode and ν is the frequency of that mode in cm^{-1}.[33]

Electronic Structure Calculations. A. Active Site Geometry. The T1 Cu site of fungal laccase was modeled by $Cu[(SCH_3)(C_3N_2H_4)_2]^+$ in C_1 symmetry, in which methyl thiolate is substituted for cysteine and imidazoles replace the histidine residues in the T1 copper coordination sphere. The crystallographic coordinates of *Coprinus cinereus* laccase[9] guided the construction of the model for the fungal laccase T1 site used in the calculations. The 1.9 Å resolution crystal structure shows a long Cu−S(Cys) distance of 2.2 Å (vide infra). Calculations were performed on a series of models with varying Cu−S_{Cys} bond lengths. Reasonable agreement with spectroscopy was given by a model with a Cu−S(Cys) bond length of 2.067 Å, the distance in the oxidized poplar plastocyanin (PLC) structure[10] (PDB code: 1PLC). The precision of this bond length in plastocyanin is ±0.04 Å.[10] The Cu−S^{γ}-C^{β} angle was placed at 110.4°, the value in the 1PLC structure. The imidazole nitrogens were placed such that the S−Cu−N angles were identical to the laccase crystal structure.[34] A coordinate system was chosen to give a Cu $d_{x^2-y^2}$ ground-state wave function;[35,36] the Cu−S(Cys) bond is 45° from the x and y axes, and the N_2S plane defines the xy plane. This axis system diagonalizes the **g** tensor for plastocyanin.[36] The Cartesian coordinates employed for calculations performed for this study are provided as Supporting Information.

B. Self-Consistent Field Xα Scattered Wave (SCF-Xα-SW) Calculations. Following the approach described in ref 23, the electronic structure of the T1 center in fungal laccase was probed using the 1982 QCPE release of the SCF-Xα-SW package.[37−40] The atomic sphere radii were adjusted to reproduce the experimentally observed g values in plastocyanin.[19] The parameters used for the SCF-Xα-SW calculations are listed as Supporting Information.

C. LCAO Density Functional Calculations. Spin-restricted calculations were performed as described in ref 23 using version 2.0.1 of the Amsterdam Density Functional (ADF) program suite.[41] Basis functions, core expansions functions, core coefficients, and fit functions for all atoms were used as provided from database IV, which includes Slater-type orbital triple-ζ basis sets for all atoms and a single-ζ polarization function for all atoms except Cu.

Results and Analysis

Identification of the Spectral Features of the T1 Cu. The absorption, CD, and MCD spectra of multicopper oxidases, including fungal laccase, are complicated by contributions from all three Cu sites. The absorption and CD spectra contain transitions involving the T1 and T3 coppers, while the MCD spectrum is a combination of transitions arising from the paramagnetic T1 and T2 coppers. To gain insight into the electronic structure of the T1 Cu, one must isolate its features from those of the T2 and T3 Cu sites. This was accomplished using the differential anion binding properties of the Cu sites. Exogenous ligands (F^-, CN^-, N_3^-, O_2^{2-}) have been shown to bind to the T2 Cu site and in some cases (N_3^- and O_2^{2-}) to bridge the T2 and T3 Cu centers.[42−46] However, the T1 Cu is

(27) Berka, R. M.; Schneider, P.; Golightly, E. J.; Brown, S. H.; Madden, M. S.; Brown, K. M.; Halkier, T.; Mondorf, K.; Xu, F. *Appl. Environ. Microbiol.* **1997**, *63*, 3151−3157.

(28) Yaver, D. S.; Xu, F.; Golightly, E. J.; Brown, K. M.; Brown, S. H.; Rey, M. W.; Schneider, P.; Halkier, T.; Mondorf, K.; Dalbøge, H. *Appl. Environ. Microbiol.* **1996**, *62*, 834−841.

(29) Wahleithner, J. A.; Xu, F.; Brown, K. M.; Brown, S. H.; Golightly, E. J.; Halkier, T.; Kauppinen, S.; Pedersen, A.; Schneider, P. *Curr. Genet.* **1996**, *29*, 395.

(30) Xu, F.; Palmer, A. E.; Yaver, D. S.; Berka, R. M.; Gambetta, G. A.; Brown, S. H.; Solomon, E. I. *J. Biol. Chem.* **1999**, *274*, 12372−12375.

(31) Felsenfeld, G. *Arch. Biochem. Biophys.* **1960**, *87*, 247−251.

(32) Carithers, R. P.; Palmer, G. *J. Biol. Chem.* **1981**, *256*, 7967−7976.

(33) Blair, D. F.; Campbell, G. W.; Schnoover, J. R.; Chan, S. I.; Gray, H. B.; Malmstrom, B. G.; Pecht, I.; Swanson, B. I.; Woodruff, W. H.; Cho, W. K.; English, A. M.; Fry, H. A.; Lum, V.; Norton, K. A. *J. Am. Chem. Soc.* **1985**, *107*, 5755−5766.

(34) The imidazole ring orientation used in the calculations was similar to that in the plastocyanin crystal structure; small deviations in ring orientation from the crystal structure of plastocyanin are due to placing the Cu in the trigonal plane.

(35) Penfield, K. W.; Gewirth, A. A.; Solomon, E. I. *J. Am. Chem. Soc.* **1985**, *107*, 4519−4529.

(36) Penfield, K. W.; Gay, R. R.; Himmelwright, R. S.; Eickman, N. C.; Norris, V. A.; Freeman, H. C.; Solomon, E. I. *J. Am. Chem. Soc.* **1981**, *103*, 4382−4388.

(37) Johnson, K. H.; Norman, J. G. J.; Connolly, J. W. D. In *Computational Methods for Large Molecules and Localized States in Solids*; Herman, F., McLean, A. D., Nesbet, R. K., Eds.; Plenum: New York, 1973; pp 161−201.

(38) Connolly, J. W. D. In *Modern Theoretical Chemistry*; Segal, G. A., Ed.; Plenum: New York, 1979; Chapter 7, pp 105−132.

(39) Rosch, N. In *Electrons in Finite and Infinite Structures*; Phariseu, P., Scheire, L., Eds.; Wiley: New York, 1977.

(40) Slater, J. C. In *The Calculation of Molecular Orbitals*; Slater, J. C., Ed.; John Wiley and Sons: New York, 1979.

(41) te Velde, G.; Baerends, E. J. *J. Comput. Phys.* **1992**, *99*, 84−98.

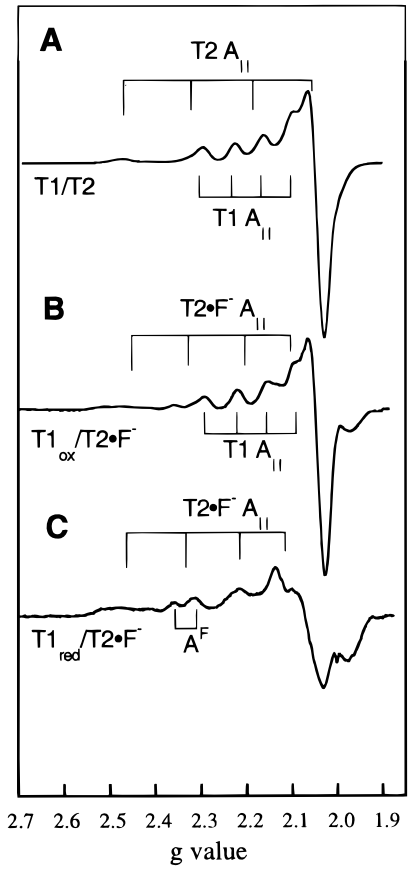

Figure 2. EPR spectrum of *Polyporus pinsitis* laccase treated with 1 equiv of F^- followed by 1 equiv of ascorbate, with the following experimental conditions: microwave frequency, 9.505 GHz; microwave power, 20 mW; modulation amplitude, 20 G; modulation frequency, 100 kHz; time constant, 0.5 s.

unaffected by exogenous ligands. Normally, the T1 Cu accepts electrons from the substrate and transfers them to the T2/T3 Cu centers in a fast ($>10^3$ s^{-1}) reaction.[1] However, binding an anion at the T2 Cu can alter the thermodynamic driving force for electron transfer from the T1 to the T2/T3 center and therefore allows selective reduction of the T1. This selective reduction of the T1 Cu allows its features to be distinguished from those of the T2 and T3 coppers. F^- binds to the T2 with high affinity,[47] and this binding can be monitored by the appearance of superhyperfine coupling between the Cu^{2+} ($S = {}^1/_2$) and the F^- ($I = {}^1/_2$). Previous studies of *Polyporus versicolor* laccase indicated that F^- binding to the T2 Cu lowers the redox potential of the T3 Cu center from 780 to 580 mV.[48] This 200 mV change in $E°$ is sufficient to localize the first electron, supplied by an external reductant, on the T1 Cu.

In the present study, P.p. laccase was treated with 1 equiv of fluoride (F^-) for 24 h. The EPR spectrum (Figure 2) of the F^--treated sample indicated that the T2 Cu features were altered,

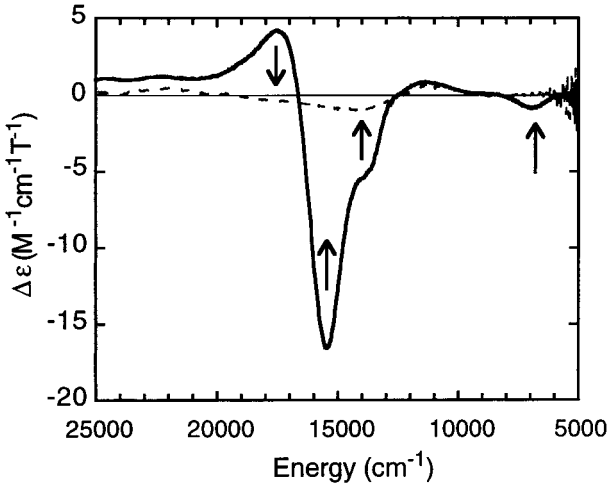

Figure 3. Magnetic circular dichroism spectra of F^--treated *Polyporus pinsitis* laccase (solid line) and F^- followed by ascorbate-treated *Polyporus pinsitis* laccase (dashed line). Samples were run at a temperature of 5 K and magnetic field of 7 T. Arrows indicate changes that occur upon addition of ascorbate (i.e., reduction of the T1 Cu).

with the appearance of ^{19}F superhyperfine coupling ($A_{||}^F = 53 \times 10^{-4}$ cm^{-1}, $A_{\perp}^F = 125 \times 10^{-4}$ cm^{-1})[49] indicating anion binding. There was no detectable change in the spin Hamiltonian parameters of the T1 Cu. Further, addition of F^- did not alter the absorption, CD, or MCD spectra. These results suggest that the T1 Cu was not significantly perturbed by F^- binding to the T2 Cu. Addition of a stoichiometric amount of ascorbate to the F^--bound sample resulted in complete loss of absorption and CD features in the visible region (see Figure S1 of Supporting Information) and disappearance of the T1 Cu EPR signal, while the F^--altered T2 Cu EPR signal remained present (Figure 2). These changes are consistent with reduction of the T1 Cu in the presence of an oxidized F^--bound T2 Cu center. Simulations show that the EPR parameters (g values, hyperfine coupling constants, and F^- superhyperfine coupling constants) of the T2 Cu in the samples containing F^-, with and without ascorbate, are the same, indicating that reduction of the T1 Cu does not affect the T2 Cu. These manipulations enable differentiation of the spectral contibutions from the T1 and T2 Cu centers.

Low-temperature MCD spectroscopy directly probes excited states of metal centers with paramagnetic ground states. Therefore, the MCD spectrum of resting P.p. laccase contains contributions from both the T1 and T2 Cu. Selective reduction of the T1 Cu allows identification of the bands due to each Cu site. Figure 3 shows the MCD spectrum of P.p. laccase + F^- ($T1_{ox}/T2{\cdot}F^-{}_{ox}$) and P.p. laccase + F^- + ascorbate ($T1_{red}/T2{\cdot}F^-{}_{ox}$). The arrows highlight the changes that occur upon addition of ascorbate. The complete loss of the negative band at 6900 cm^{-1} and the positive feature ~17 500 cm^{-1} upon T1 reduction indicates these bands arise from the T1 Cu. In addition, the negative bands ~13 500 and ~15 500 cm^{-1} lose most of their intensity, suggesting that the T1 Cu makes a significant contribution in this region. The spectrum of P.p. laccase + F^- + ascorbate has a positive MCD feature at ~11 000 cm^{-1} and a negative feature at ~15 000 cm^{-1}. These MCD transitions are consistent with previous reports of the T2 Cu MCD spectrum in *Rhus vernicifera* (tree) laccase where the T2 features were selectively observed by replacing the T1 Cu with spectroscopically innocent Hg^{2+}.[44]

(42) Fee, J. A.; Malkin, R.; Malmström, B. G.; Vänngård, T. *J. Biol. Chem.* **1969**, *244*, 4200−4207.
(43) Malkin, R.; Malmström, B. G.; Vänngård, T. *Eur. J. Biochem.* **1969**, *10*, 324−329.
(44) Cole, J. L.; Clark, P. A.; Solomon, E. I. *J. Am. Chem. Soc.* **1990**, *112*, 9534−9548.
(45) Spira-Solomon, D. J.; Solomon, E. I. *J. Am. Chem. Soc.* **1987**, *109*, 6421−6432.
(46) Sundaram, U. M.; Zhang, H. H.; Hedman, B.; Hodgson, K. O.; Solomon, E. I. *J. Am. Chem. Soc.* **1997**, *119*, 12525−12540.
(47) Brändén, R.; Malmström, B. G.; Vänngård, T. *Eur. J. Biochem.* **1973**, *36*, 195−200.
(48) Reinhammar, B. R. M. *Biochim. Biophys. Acta* **1972**, *275*, 245−259.

(49) Although the splittings are clearly observed in the spectrum, superhyperfine coupling constants were obtained from EPR simulations.

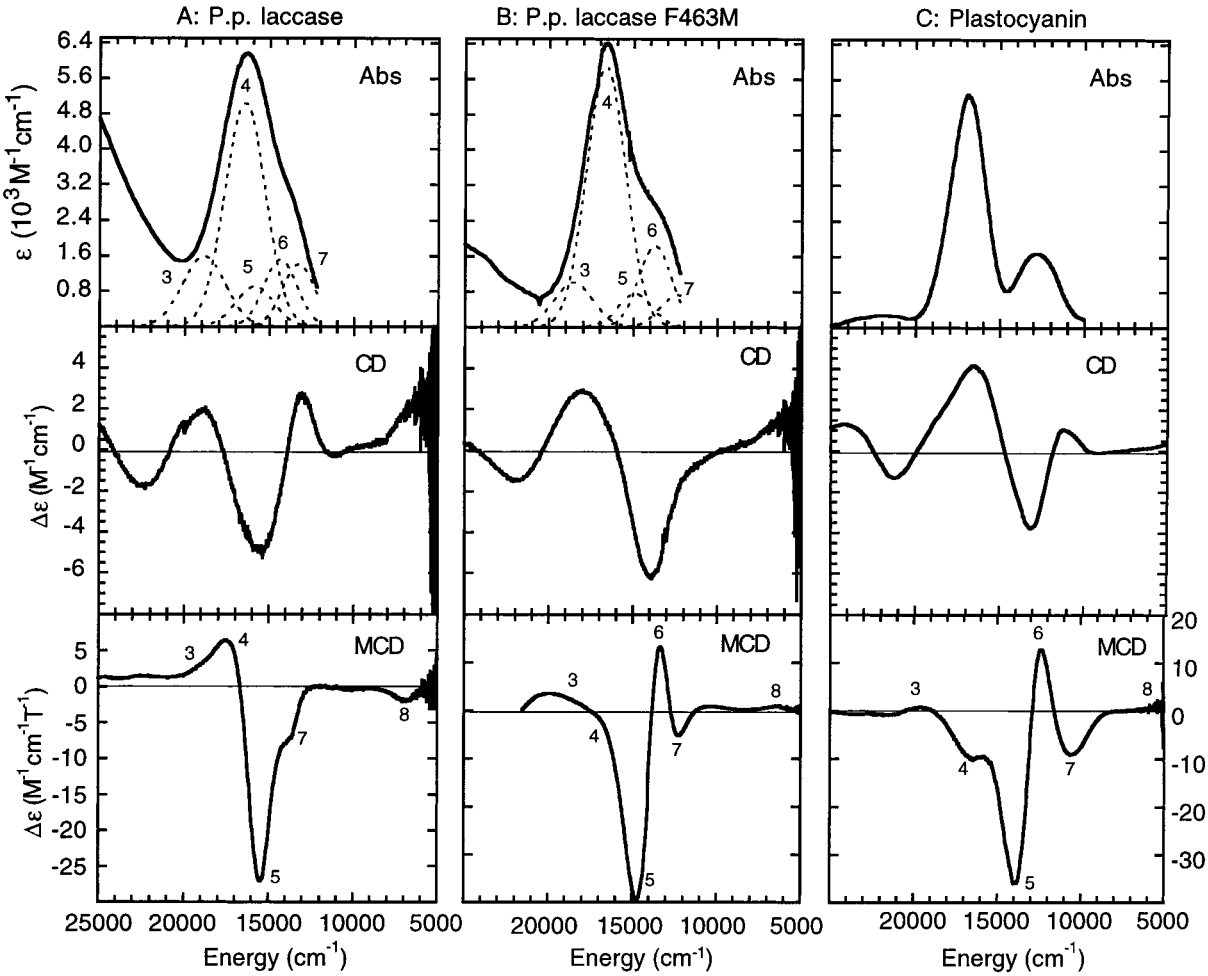

Figure 4. Room-temperature electronic absorption (top), room-temperature circular dichroism (CD), and low-temperature (5 K) magnetic circular dichroism spectra of *Polyporus pinsitis* laccase (A), the *Polyporus pinsitis* laccase F463M mutant (B), and plastocyanin[19] (C).

Table 2. Experimental Spectroscopic Parameters for M.t., R.s., P.p., and the P.p. F463M Laccase

		energy (cm^{-1})					oscillator strength (f_{exp})				
band		M.t.	R.s.	P.p.	P.p. F463M	PLC[a]	M.t.	R.s.	P.p.	P.p. F463M	PLC[d]
8	d_{z^2}	6 500[b]	6 500[b]	6 900[b]	6 500[b]	5 000[b]	*c*	*c*	*c*	*c*	*c*
7	d_{xy}	13 160	13 080	13 270	12 370	10 800	0.0105	0.0112	0.0122	0.0068	0.0066
6	d_{yz}	14 290	14 590	14 350	13 700	12 800	0.0134	0.0152	0.0136	0.0164	0.0126
5	d_{xz}	15 470	15 850	15 860	14 880	13 950	0.0071	0.0094	0.0092	0.0069	0.0049
4	S π	16 610	16 660	16 450	16 630	16 700	0.0576	0.0502	0.0555	0.0626	0.0501
3	S pseudo-σ	18 650	18 640	18 860	18 540	18 700	0.0210	0.0186	0.0183	0.0105	0.0082
							0.1096	0.1046	0.1088	0.1032	0.0824

[a] Parameters for plastocyanin were reported previously in ref 23. [b] The energy of the d_{z^2} transition is taken from the low-temperature MCD, whereas the energies of the remainder of the transitions are taken from room-temperature absorption. [c] The oscillator strength of this transition could not be calculated because the absorption ϵ_{max} was not determined. [d] The oscillator strength of the room-temperature spectrum of plastocyanin is reported in order to compare with the room-temperature data on the fungal laccases.

Absorption/CD/MCD. The MCD spectral features of the T1 Cu in P.p. laccase were obtained by subtracting the spectrum of P.p. laccase + F^- + ascorbate ($T1_{red}/T2{\cdot}F^-_{ox}$) from the spectrum of P.p. laccase + F^- ($T1_{ox}/T2{\cdot}F^-_{ox}$). The room-temperature absorption, CD, and low-temperature (5 K) MCD spectra of the T1 Cu in P.p. laccase obtained in this manner are shown in Figure 4A. Simultaneous fitting of these three spectra revealed that six bands were required to fit the region from 5000 to 25 000 cm^{-1}.[50] These bands are depicted by the dashed lines in the absorption spectrum. To be consistent in our comparison with other blue copper proteins, we have used the numbering scheme from plastocyanin.[19] The experimental oscillator strengths (f_{exp}) were calculated according to the approximation $f_{exp} \approx 4.61 \times 10^{-9} \epsilon_{max} \nu_{1/2}$, where the absorption maximum (ϵ_{max}) is expressed in M^{-1} cm^{-1} and the full width at half-maximum ($\nu_{1/2}$) is expressed in cm^{-1}. The energies and experimental oscillator strengths of the bands are given in Table 2. The absorption, CD, and MCD spectra of M.t. laccase and R.s. laccase are very similar to those of P.p. laccase and are presented in Supporting Information (Figures S2 and S3). The transition energies and experimental oscillator strengths of all three enzymes are included in Table 2.

In addition to studying the wild-type fungal laccases, we examined a mutant in which the nonligating axial Phe in P.p. laccase was changed to a Met.[30] Figure 4B displays the absorption, CD, and MCD of the P.p. laccase F463M mutant.

(50) The energy region above 25 000 cm^{-1} is obscured by contributions from a small heme impurity.

Again, the individual Gaussian resolved transitions obtained from simultaneous fitting of the absorption, CD, and MCD spectra are given by the dashed lines in the absorption spectrum. The energies and experimental osciallator strength of the bands are included in Table 2.

Ligand field and charge-transfer transitions can be differentiated by comparing their relative intensities in absorption and MCD. In particular, the MCD intensity depends on the magnitude of spin−orbit coupling for the center involved in the transition.[51−53] Because the spin−orbit coupling parameter for Cu is greater than that for S or N (ξ_{3d}(Cu) ≈ 828 cm^{-1}, ξ_{3p}(S) ≈ 382 cm^{-1}, ξ_{2p}(N) ≈ 70 cm^{-1}), transitions centered on the Cu (i.e., d → d) have a higher *C*-term MCD intensity than transitions involving significant S or N character (i.e., charge transfer). Alternatively, absorption intensity is expected to be much higher for charge transfer (CT) transitions because the ligand−ligand overlap (which determines absorption intensity) between the two states involved in the charge-transfer transition should be much larger.

In both the wild-type P.p. laccase and the F463M mutant, band 4 at ∼16 500 cm^{-1} (∼600 nm) has a very high absorption ϵ_{max} and a relatively low MCD intensity and is the intense feature responsible for the blue color of fungal laccase. In analogy with other well-characterized blue copper proteins[19,23,21] (Figure 4, Table 2) this band involves a π-type Cu−S_{Cys} bonding interaction and is thus assigned as a S π → Cu $d_{x^2-y^2}$ CT transition. Note that EPR and density functional calculations identify $d_{x^2-y^2}$ as the highest occupied molecular orbital (HOMO) (vide infra). Band 3 can also be assigned a S → Cu $d_{x^2-y^2}$ CT transition but as shown previously,[19,54] it is characterized by a pseudo-σ bonding interaction. There has been some disagreement as to whether a band is in fact present in the 18 800 cm^{-1} energy region;[55,56] however, our data, particularly the CD spectrum, show that it is indeed required to be present on the basis of experiment. Although these two S_{Cys} → Cu $d_{x^2-y^2}$ CT transitions are at similar energies in the fungal laccases, in the P.p. laccase F463M mutant, and in plastocyanin, the oscillator strength of the charge-transfer transitions varies significantly. The total oscillator strength at room temperature in the fungal laccases ranges from 0.1046 to 0.1096, which is about 30% higher than in plastocyanin (0.0824). The oscillator strength observed in P.p. laccase F463M (0.1032) is about 5% lower than in the wild type but higher than for plastocyanin. The oscillator strength of a ligand-to-metal charge-transfer transition can be correlated with the donor strength of the ligand.[57] A higher oscillator strength in fungal laccase thus indicates that the Cu−S_{Cys} bond is stronger and more covalent in the fungal laccases. The decrease in oscillator strength in the F463M mutant demonstrates that the covalency of the Cu−S_{Cys} bond is lowered relative to the wild type. The larger covalency of the fungal laccase T1 center observed here is further supported by Q band electron nuclear double resonance (ENDOR) measurements[58] of the β-methylene ^{1}H hyperfine couplings (HFCs) for the Cys residue ligated to the Cu center. In this comparative study of T1 sites, different blue Cu centers gave similar ρ_S values with the exception of a fungal laccase where the spin density (and therefore covalency) was ∼33% larger.[59] Sulfur K-edge (S 1s → S 3p) X-ray absorption spectroscopy can provide a direct, quantitative measure of the S covalency of the HOMO, and these studies are currently being pursued.

The four lower energy transitions observed in the optical spectra of wild type and F463M P.p. laccase (bands 5−8) are assigned to ligand field transitions. On the basis of MCD sign and intensity, band 5 is attributed to the d_{xz}→ $d_{x^2-y^2}$ transition; this transition is typically the most intense negative feature in the blue copper MCD spectrum.[19,21,23] Band 6 is not resolved in the P.p. laccase MCD spectrum; however, its presence is required by the simultaneous fit of the absorption, CD, and MCD spectra. Presumably, band 6 is not resolved in the MCD spectrum because it overlaps the negative bands resulting from the d_{xz} → $d_{x^2-y^2}$ and d_{xy} → $d_{x^2-y^2}$ transitions, since these bands are very close in energy in fungal laccase. However, band 6 is clearly resolved in the P.p. laccase F463M MCD spectrum, and because of its positive sign, it is attributed to the d_{yz} → $d_{x^2-y^2}$ transition. On the basis of analysis of the MCD sign and comparison to other blue copper proteins (vide infra), band 7 is assigned as d_{xy} → $d_{x^2-y^2}$ and band 8 is attributed to d_{z^2} → $d_{x^2-y^2}$.

Overall, there are several important spectral differences among the fungal laccases, the F463M mutant, and plastocyanin, which serves as a reference point for describing blue copper centers (Figure 4, Table 2). In the fungal laccases, the d → d bands shift to a higher transition energy than in plastocyanin. This is most clearly manifested in the absorption spectrum in which the d → d bands appear as a shoulder at 13 700 cm^{-1}. In plastocyanin these bands exhibit a well-resolved envelope at ∼12 500 cm^{-1}. The electronic spectra of the F463M mutant, where the nonligating Phe was replaced with a potentially ligating Met, reveal that the d → d bands are lower in energy than in the wild type but higher than in plastocyanin. Further, the d_{xz}, d_{yz}, and d_{xy} transitions are grouped closer in energy in the fungal laccases; thus, the d_{yz} → $d_{x^2-y^2}$ transition is not clearly resolved in the MCD spectrum. In the F463M mutant, these bands are more spread out in energy (Figure 4B), allowing the positive MCD band 6, the d_{yz} → $d_{x^2-y^2}$ transition, to be observed. In plastocyanin, these bands are still further separated in energy.

In the wild-type fungal laccases, the lowest energy transition (d_{z^2} → $d_{x^2-y^2}$) is negative, whereas in the F463M mutant and other axially ligated blue copper proteins it is positive.[19,21,23] The origin of this sign change can be understood by examining the different mechanisms of the MCD *C*-term intensity. As mentioned earlier, for a transition to have *C*-term intensity it must be polarized in two perpendicular directions. In the low-symmetry blue copper site this is accomplished by spin−orbit

(51) Piepho, S. B.; Schatz, P. N. In *Group Theory in Spectroscopy—With Applications to Magnetic Circular Dichroism*; Piepho, S. B., Schatz, P. N., Eds.; John Wiley and Sons: New York, 1983.

(52) Gerstman, B. S.; Brill, A. S. *J. Chem. Phys.* **1985**, *82*, 1212−1230.

(53) MCD intensity of Cu^{2+} at low temperature arises from *C*-terms. *C*-term intensity requires polarization in two perpendicular directions. However, the low symmetry of the blue copper site removes all orbital degeneracy; therefore, transitions are polarized in only one direction. For low-symmetry sites, the only mechanism for *C*-term intensity involves spin−orbit coupling between states that mix their orthogonal polarizations.

(54) Lu, Y.; Lacroix, L. B.; Lowery, M. D.; Solomon, E. I.; Bender, C. J.; Peisach, J.; Roe, J. A.; Gralla, E. B.; Valentine, J. S. *J. Am. Chem. Soc.* **1993**, *115*, 5907−5918.

(55) Pierloot, K.; De Kerpel, J. O. A.; Ryde, U.; Roos, B. O. *J. Am. Chem. Soc.* **1997**, *119*, 218−226.

(56) Pierloot, K.; De Kerpel, J. O. A.; Ryde, U.; Olsson, M. H. M.; Roos, B. O. *J. Am. Chem. Soc.* **1998**, *120*, 13156−13166.

(57) Baldwin, M. D.; Root, D. E.; Pate, J. E.; Fujisawa, K.; Kitajima, N.; Solomon, E. I. *J. Am. Chem. Soc.* **1992**, *114*, 10421−10431.

(58) Werst, M. M.; Davoust, C. E.; Hoffman, B. M. *J. Am. Chem. Soc.* **1991**, *113*, 1533−1538.

(59) We note that by using the appropriate McConnell relation (i.e., $A \approx \rho_S Q^{SCH} \cos^2\theta$) with the Cu−$S^{\gamma}$−$C^{\beta}$−$H^{\beta}$ dihedral angles derived from the crystal structure,[10] and a value of Q^{SCH} (83 MHz) appropriate for a S-centered radical,[79] and the orientation of the orbital containing the unpaired spin known from single-crystal EPR,[35] the spin density at the thiolate S can be estimated for plastocyanin to give ρ_S = 0.36 (in good agreement with the Xα-SW and S K-edge XAS value of ∼38%[17]).

coupling, which mixes transitions of orthogonal polarization. Both excited state and ground-state spin−orbit (s−o) coupling can contribute to the overall *C*-term intensity. The former leads to the MCD sum rule that the *C*-term intensity summed over all excited states must equal zero, while the latter leads to deviations from the sum rule. The contributions of both these mechanisms are summarized in the following equation:[60]

$$\bar{C}_o = -\frac{1}{12}\sum_{\substack{j\neq i\\ \text{doubly}}}\sum_{uvw}\epsilon_{uvw}g_w \{\Delta_j^{-1}\,\mathrm{Im}\langle\psi_o|\sum_N\xi(r_N)\vec{l}_{N,w}|\psi_j\rangle\langle\psi_i|\vec{r}_u|\psi_o\rangle\langle\psi_j|\vec{r}_v|\psi_i\rangle + \Delta_{j,i}^{-1}\,\mathrm{Im}\langle\psi_i|\sum_N\xi(\vec{r}_N)\vec{l}_{N,w}|\psi_j\rangle\langle\psi_o|\vec{r}_u|\psi_j\rangle\langle\psi_i|\vec{r}_v|\psi_o\rangle\} \quad (1)$$

where the first term in braces represents the ground-state s−o coupling and the second term denotes the excited-state s−o coupling. In this equation, o denotes the acceptor orbital (i.e., the ground state), *i* denotes the donor orbital (i.e., the excited state), and *j* denotes an intermediate orbital (i.e., an intermediate excited state).[61]

Using this equation and the procedure described in ref 60, we can analyze the individual contributions to the *C*-term intensity of the $d_{z^2} \rightarrow d_{x^2-y^2}$ transition for fungal laccase and for plastocyanin. In this case, the donor orbital (excited state) is d_{z^2}, the acceptor orbital (ground state) is $d_{x^2-y^2}$, and the intermediate orbital is either d_{xy}, d_{xz}, d_{yz}, S_{Cys} π, or S_{Cys} pseudo-σ.[62] For plastocyanin, the $d_{z^2} \rightarrow d_{x^2-y^2}$ transition is calculated to be positive. The main contribution to this positive intensity is excited-state spin−orbit coupling with d_{yz}, which involves the L_x operator coupling m_z and m_y polarized transitions. In fungal laccase, m_z decreases significantly to the point where it is negligible. This derives from the lack of an axial ligand that drops the Cu atom into the N_2S plane, eliminating the transition density in the *z* direction, which is perpendicular to the plane.

EPR Spectra and Parameters. Figure 5 shows the EPR spectra and simulations for the three fungal laccases and the P.p. laccase F463M mutant. Table 3 presents the spin Hamiltonian parameters obtained from EPR spectral simulations. The observed *g* values ($g_{||} > g_{\perp} > 2.0023$) are consistent with a $d_{x^2-y^2}$ half-occupied highest molecular orbital (HOMO). In all three fungal laccases, $g_{||}$ is significantly smaller than in plastocyanin (2.208−2.194 vs 2.226). There are no significant differences in the spin Hamiltonian parameters of the three fungal laccases. In the F463M mutant, the $g_{||}$ value (2.213) is between that of the wild-type enzyme and plastocyanin. Similarly, the $g_{\perp}$ value of the three fungal laccases and the P.p. laccase F463M mutant is smaller than that observed in plastocyanin. The *g* value expressions obtained from ligand field theory are directly proportional to the amount of metal character in the half-occupied HOMO (i.e., covalency) and inversely proportional to the ligand field transition energies.[63] Analyses of d → d bands in the absorption, CD, and MCD spectra reveal that the ligand field transitions have shifted higher in energy in the fungal laccases relative to plastocyanin. Assuming a similar covalency for plastocyanin and the T1 site in fungal laccase, the following expressions can be used to estimate the *g* value dependence on the ligand field transition energies.

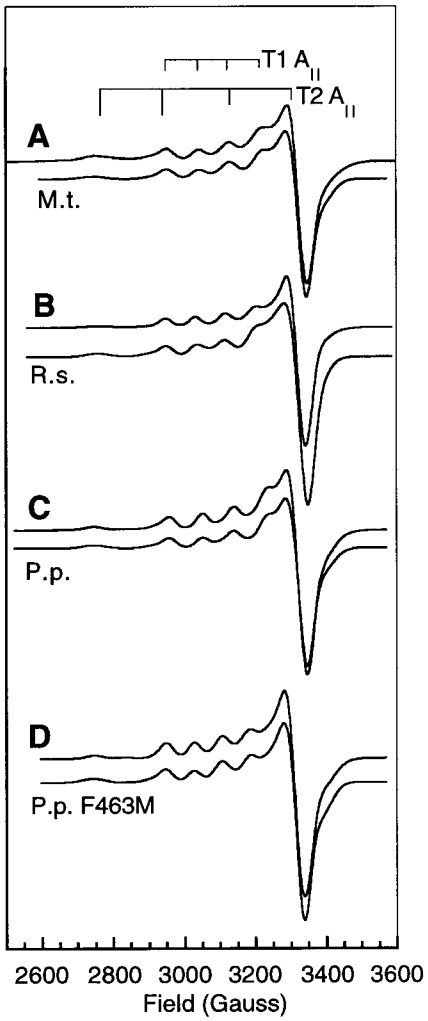

Figure 5. EPR spectra of *Myceliophthora thermophila* laccase (A), *Rhizoctonia solani* laccase (B), *Polyporus pinsitis* laccase (C), and *Polyporus pinsitis* F463M (D). Experimental conditions are the following: microwave frequency, 9.505 GHz; microwave power, 20 mW; modulation amplitude, 20 G; modulation frequency, 100 kHz; time constant, 0.5 s.

Table 3. Spin Hamiltonian Parameters Obtained from EPR Simulations

	T1 Cu				T2 Cu	
	$g_{||}$	$A_{||}$	$g_{\perp}$	A	$g_{||}$	$A_{||}$
M.t.	2.201	87	2.045	7	2.247	185
R.s.	2.208	82	2.043	10	2.265	160
P.p.	2.194	90	2.046	8	2.248	182
P.p. F463M	2.213	78	2.047	9	2.248	183
plastocyanin[a]	2.226	63	2.053	17		

[a] Published previously in ref 35.

(60) Neese, F.; Solomon, E. I. *Inorg. Chem.* **1999**, *38*, 1847−1865.

(61) The ground-state s−o coupling contribution to the *C*-term MCD contains three components: (1) Δ_j^{-1}, the transition energy of the intermediate excited state, (2) the cross product of the polarization of the ground state → excited-state transition with the polarization of the excited state → intermediate excited-state transition, and (3) the spin−orbit coupling of the intermediate excited state and the ground state. Likewise, the excited-state s−o coupling contains three components: (1) $\Delta_{j,i}^{-1}$, the transition energy of the intermediate excited state minus the transition energy of the excited state, (2) the cross product of the polarization of the ground state → intermediate excited-state transition with the polarization of the ground state → excited-state transition, and (3) the spin−orbit coupling of the intermediate excited state and the excited state.

(62) The transition polarizations were obtained from the product of the wave function coefficients of the ligand components of the appropriate molecular orbitals (obtained from Xα-SW calculations, vide infra) oriented along the ligand Cartesian coordinates and summed over all ligands. Δ^{-1} was determined from the experimental transition energies and L_i were calculated for the appropriate d-orbtials. This is given by the covalency (obtained from Xα) × the Cu s−o coupling contant (830 cm^{-1}) × the angular momentum matrix element.

(63) McGarvey, B. R. In *Transition Metal Chemistry*; Carlin, B. L., Ed.; 1966; Chapter 3, pp 89−201.

$$\Delta g_{\|}(\text{laccase}) = \frac{E_{xy}(\text{PLC})}{E_{xy}(\text{laccase})}\Delta g_{\|}(\text{PLC}) \quad (2)$$

$$\Delta g_{\perp}(\text{laccase}) = \frac{E_{xz,yz}(\text{PLC})}{E_{xz,yz}(\text{laccase})}\Delta g_{\perp}(\text{PLC}) \quad (3)$$

In these equations, $\Delta g_{\|\perp}$ is the deviation of that g value from the spin-only value (2.0023) and E is the experimental transition energy in cm^{-1}. Using these expressions, the experimental energies of the $d_{xy} \rightarrow d_{x^2-y^2}$ transitions (E_{xy}), and $g_{\|}$ of plastocyanin (see Table 2 for values), $g_{\|}$ for the T1 site is predicted to be 2.186 for M.t., 2.187 for R.s., 2.184 for P.p., and 2.197 for the P.p. F463M mutant. These calculated values are in close agreement with, but are all lower than, the experimental values. However, it should also be noted that these calculated values will increase slightly when the experimentally derived covalency (vide supra) is taken into consideration. When $E_{xz,yz}$ is used, $g_{\perp}$ of the laccases is predicted to be 2.046 for M.t., 2.045 for R.s., 2.045 for P.p., and 2.047 for the P.p. F463M mutant. The calculated values for the T1 Cu in all three fungal laccases and the F463M mutant are quite similar to the experimental ones, indicating that the increased ligand field transition energies account for the smaller g values in these enzymes.

Relative to plastocyanin, the $A_{\|}$ value is higher in the fungal laccases ($|63| \times 10^{-4}$ cm^{-1} for plastocyanin vs $(|82-90|) \times 10^{-4}$ cm^{-1}), while that of the P.p. laccase F463M axial mutant ($|78| \times 10^{-4}$ cm^{-1}) is between that of the wild-type P.p. laccase and that of plastocyanin. The $A_{\perp}$ values are too small to be obtained reliably. The hyperfine coupling constant depends on several competing factors, including (a) Fermi contact, which results from unpaired spin density at the Cu nucleus, (b) direct spin dipolar coupling, which arises from the interaction of the electron spin (S) with the nuclear spin (I) of the metal, and (c) indirect (orbital) dipolar coupling, which occurs as a result of coupling between the electron orbital magnetic moment (L) and the nuclear spin (I) of the metal. The following ligand field expressions are used to describe these contributions to the hyperfine coupling:[63]

$$A_{\|} = P_{\text{d}}\left(-\kappa - \frac{4}{7}\alpha^2 + \frac{3}{7}\Delta g_{\perp} + \Delta g_{\|}\right) \quad (4)$$

$$A_{\perp} = P_{\text{d}}\left(-\kappa + \frac{2}{7}\alpha^2 + \frac{11}{14}\Delta g_{\perp}\right) \quad (5)$$

where P_{d} is 396×10^{-4} cm^{-1}, κ is the Fermi contact term, and α^2 is the percent metal character in the $d_{x^2-y^2}$ orbital. If we make the reasonable assumptions that κ and α^2 are the same in the fungal laccases and plastocyanin and that the hyperfine coupling is negative,[64] experimental g values can be used to calculate the hyperfine coupling. The lower values of $\Delta g_{\|}$ and $\Delta g_{\perp}$ in the fungal laccases relative to plastocyanin will decrease the indirect orbital dipolar contribution to the hyperfine. Because the indirect dipolar contribution is positive, a decrease in this term will result in the hyperfine becoming more negative (i.e., larger in magnitude). When the experimental g values are used, the value of $A_{\|}$ changes from -63×10^{-4} cm^{-1} for plastocyanin to -74×10^{-4} cm^{-1} for M.t. laccase, -71×10^{-4} cm^{-1} for R.s. laccase, -76×10^{-4} cm^{-1} for P.p. laccase, and -69×10^{-4} cm^{-1} for P.p. F463M. Thus, the decrease in g values accounts for about 50% of the difference in hyperfine coupling between plastocyanin and fungal laccase. Another possible contribution to the difference in hyperfine couplings could be a change in 4s mixing into the HOMO. The contribution of 4s to the Fermi contact term is large and positive. Therefore, even a small decrease in 4s mixing would cause the hyperfine coupling to become more negative. Density functional calculations (vide infra) on fungal laccase indicate that the amount of 4s mixing does indeed decrease from 1% in plastocyanin[23] to 0% in fungal laccase because of the planar geometry of fungal laccase. This decrease would result in the hyperfine coupling becoming more negative by about 16.8×10^{-4} cm^{-1} in the fungal laccases. When combined with the change in ligand field, these contributions predict a parallel hyperfine coupling of -91×10^{-4} cm^{-1} for M.t.L, -87×10^{-4} cm^{-1} for R.s.L, and -93×10^{-4} cm^{-1} for P.p.L, in reasonable agreement with the experimentally observed values. The value of -69×10^{-4} cm^{-1} predicted for F463M P.p. laccase follows the anticipated trend based on ligand field transition energies; however, it is lower than the experimentally observed value of $|78| \times 10^{-4}$ cm^{-1}. The predicted $A_{\|}$ value cannot be corrected for the change in 4s mixing because no structure is available for electronic structure calculations.

(64) The sign of the hyperfine parameter cannot be determined from a typical EPR experiment, but single-crystal studies[35] and calculations indicate that it is negative.

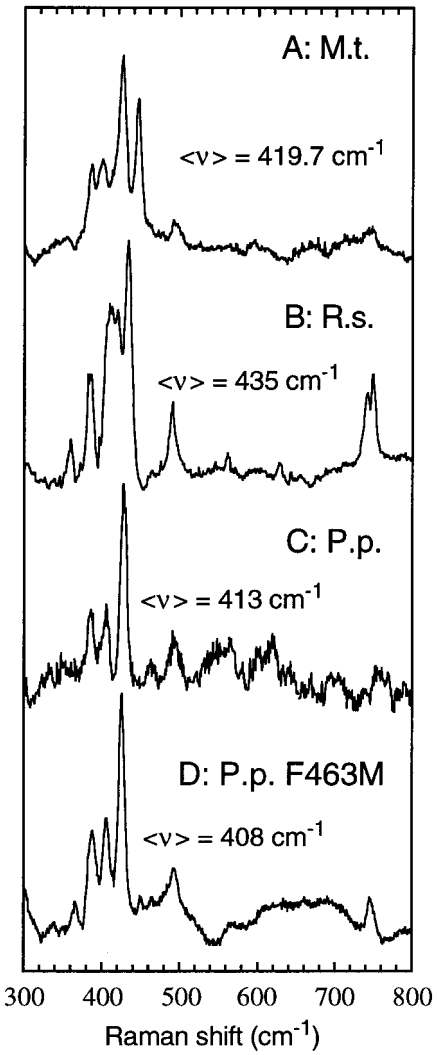

Figure 6. Resonance Raman spectra obtained upon excitation at 647.1 nm for *Myceliophthora thermophila* laccase (A), *Rhizoctonia solani* laccase (B), *Polyporus pinsitis* laccase (C), and *Polyporus pinsitis* F463M (D).

Resonance Raman. Figure 6 presents the resonance Raman spectra of the three fungal laccases and the PpL F463M mutant

Table 4. SCF-Xα-SW Description of the T1 Cu Site in Fungal Laccase

			% Cu														
				l breakdown			d m_l breakdown					% Cys		% Im B		% Im A	
level	label	energy (eV)	Cu	s	p	d	x^2-y^2	xz	z^2	yz	xy	S^γ	Cys	N^δB	His B	N^δA	His A
38 a	x^2-y^2	−4.186	54	0.0	0.5	52.9	52.29	0.12	0.02	0.02	0.47	37	4	2	0	2	0
37 a	xy	−4.848	81	4.9	6.5	68.9	0.02	0.28	6.79	3.28	58.48	13	1	1	1	1	1
36 a	z^2	−5.435	91	2.7	0.0	87.4	0.09	15.69	61.91	1.66	8.01	1	0	1	0	2	5
35 a	xz	−5.474	85	0.0	0.0	84.2	0.36	61.20	19.92	2.34	0.33	3	1	0	0	2	9
34 a	yz	−5.563	93	0.0	0.0	93.0	0.07	1.83	1.20	83.00	6.90	1	1	1	3	0	0
33 a	ImA π_1	−5.936	21	0.0	1.5	18.9	2.64	14.57	0.07	0.14	1.47	7	0	0	0	6	63
32 a	S_{Cys} π	−6.117	46	0.0	4.6	39.1	38.19	0.15	0.06	0.02	0.67	38	4	1	0	2	8
31 a	ImB π_1	−6.352	4	0.0	0.3	3.4	0.04	0.09	0.00	3.22	0.05	0	0	6	89	0	0
30 a	S_{Cys} pseudo-σ	−7.464	28	1.7	3.6	21.0	0.06	3.84	2.35	3.16	11.60	61	11	0	0	0	0
29 a	ImA π_2	−8.47	4	0.2	0.7	2.5	0.12	1.20	0.08	0.00	1.11	0	0	0	0	52	43
28 a	ImB π_2	−9.629	6	0.0	0.9	3.6	0.10	0.07	0.00	2.70	0.72	0	0	53	42	0	0
27 a	S_{Cys} σ	−10.705	26	1.8	10.9	10.1	0.45	0.10	0.97	0.14	8.49	44	23	0	0	5	0

obtained with excitation at 647.1 nm into the $S_{Cys} \rightarrow$ Cu charge-transfer band. As for other blue copper proteins,[33,65] the spectra are characterized by a complex envelope of rR bands centered around 400 cm^{-1}, all of which are associated with Cu−S vibrations. In all of the fungal laccases, the envelope of bands occurs at higher frequency than plastocyanin.[33] The most intense peak in the resonance Raman spectrum varies as follows: 428 cm^{-1} (M.t. laccase), 435 cm^{-1} (R.s. laccase), 428 cm^{-1} (P.p. laccase), and 426 cm^{-1} (F463M mutant) compared to 425 cm^{-1} for plastocyanin[33] and 408 cm^{-1} for *P. aeruginosa* azurin.[66] The intensity-weighted average, $\langle \nu_{Cu-S} \rangle$, of the peaks in the 400 cm^{-1} envelope has been shown to be an indicator of the Cu−S_{Cys} bond strength as described in ref 33. For the fungal laccases the following values of $\langle \nu_{Cu-S} \rangle$ were obtained: 419.7 cm^{-1} (M.t. laccase), 435.7 cm^{-1} (R.s. laccase), 413 cm^{-1} (P.p. laccase), and 407.6 cm^{-1} (P.p. laccase F463M). These results indicate that the wild-type fungal laccases have a stronger Cu−S_{Cys} bond than plastocyanin ($\langle \nu_{Cu-S} \rangle = 403$ cm^{-1})[33] or *P. aeruginosa* azurin ($\langle \nu_{Cu-S} \rangle = 405$ cm^{-1}).[33] The increase in the strength of the Cu−S_{Cys} interaction from the Raman data is in agreement with the increased oscillator strength observed in the fungal laccases (vide supra) and the ENDOR data.[58] The $\langle \nu_{Cu-S} \rangle$ of P.p.L decreases upon mutation of the axial F to M, and the observed $\langle \nu_{Cu-S} \rangle$ is much closer to the $\langle \nu_{Cu-S} \rangle$ found in blue Cu proteins with a $(his)_2(cys)(met)$ coordination sphere.

Electronic Structure Calculations. Xα-SW electronic structure calculations were performed to gain further insight into the origin of the differences between the electronic structure of the T1 center in fungal laccase and plastocyanin. The ground-state energies and one-electron wave functions are summarized in Table 4. Plots of the contours of the HOMO both perpendicular and parallel to the N_2S plane are displayed in Figure 7.

The electronic structural properties of the HOMO are important, since this orbital is associated with the electron transfer reactivity of this site. Table 4 and Figure 7 suggest that the HOMO of the T1 center in fungal laccase is highly covalent, containing only 54% Cu character.[67] The majority of the remaining orbital character comes from S_{Cys} (37%). The S

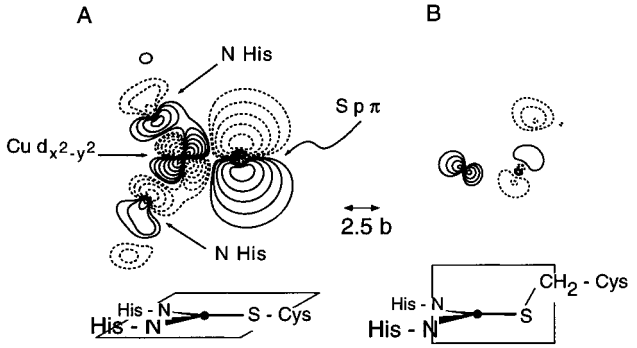

Figure 7. Contours of the half-filled HOMO (level 37a) of fungal laccase plotted parallel (A) and perpendicular (B) to the N_2S plane. Contours are at ±0.64, ±0.32, ±0.16, ±0.08, ±0.04, ±0.02, and ±0.01 $(e/bohr)^{1/2}$.

character in the HOMO is characterized by a π-type S_{Cys}−Cu interaction between the Cu $d_{x^2-y^2}$ orbital and the S pπ orbital, a situation very similar to that observed for plastocyanin.[19,23,55,68] The calculated S_{Cys} character in the HOMO of the T1 in fungal laccase (37%) corresponds to a 2% increase from the amount of S character in the HOMO of plastocyanin (35%).[23,69] The small increase in S_{Cys} character in the HOMO of fungal laccase, relative to plastocyanin, is consistent with the higher oscillator strength (vide supra), the increased S_{Cys} spin density implied from the β-methylene ^1H proton hyperfine couplings observed with ENDOR (vide supra),[58] and the increased $\langle \nu_{Cu-S} \rangle$ obtained from resonance Raman data. While the increase in thiolate character predicted by the calculations is smaller than the experimentally observed increase, the calculations clearly show that the increase derives from the loss of the axial Met ligand in fungal laccase (vide infra). Finally, the calculation reveals that relative to plastocyanin, there is a decrease in 4s mixing into the HOMO in fungal laccase (1% vs 0%), which contributes to the larger $A_{||}$ value observed for fungal laccase (vide supra).

(65) Han, J.; Adman, E. T.; Beppu, T.; Codd, R.; Freeman, H. C.; Huq, L.; Loehr, T. M.; Sanders-Loehr, J. *Biochemistry* **1991**, *30*, 10904−10913.

(66) Andrew, C. R.; Yeom, H.; Valentine, J. S.; Karlsson, B. G.; Bonander, N.; van Pouderoyen, G.; Canters, G. W.; Loehr, T. M.; Sanders-Loehr, J. *J. Am. Chem. Soc.* **1994**, *116*, 11489−11498.

(67) This is in contrast to the 42% Cu character in plastocyanin determined experimentally from Cu L-edge spectroscopy. The difference between the calculated and experimental Cu character most likely relates to the effects of charge partitioning in the intersphere region and sphere overlap in the calculations.

(68) Larsson, S.; Broo, A.; Sjölin, L. *J. Phys. Chem.* **1995**, *99*, 4860−4865.

(69) The value of 38% for the S character in plastocyanin originated from the calculations of ref 19, which used a C_s-idealized Cu site with a Cu−S(Cys) distance of 2.13 Å. These calculations were experimentally calibrated to the EPR *g*-values by varying the sphere radii. For accurate comparison with the C_1 fungal laccase site, we use the plastocyanin calculations of LaCroix et al.[23] These calculations employ the same sphere radii as Gewirth and Solomon (and the present study), a Cu−S(Cys) distance of 2.067 Å, and a C_1 representation of the plastocyanin active site. These more recent plastocyanin Xα-SW calculations give a value of 35% for the S character in the HOMO of plastocyanin. The quantitative difference (3%) in S character between these two plastocyanin calculations is due to differences in charge partitioning in the intersphere regions and differences in sphere overlap.

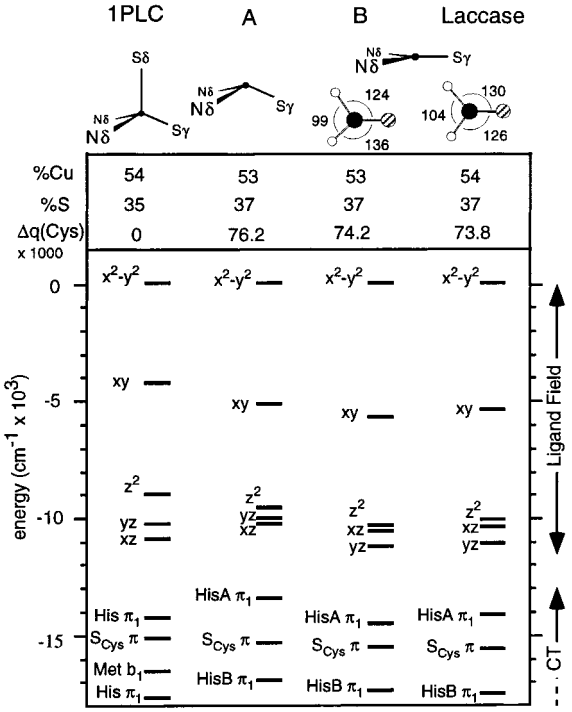

Figure 8. Density functional correlation of the one-electron energies for plastocyanin, fungal laccase, and intermediate structure models. The geometries are described in the text. Top two numbers represent Cu and S character in the HOMO. Δq(Cys) denotes the change ($\times 1000$) on all atoms of the Cys residue relative to plastocyanin, as calculated by ADF. The energy level diagrams have been aligned with the $x^2 - y^2$ orbital at zero energy.

The four remaining fully occupied d orbitals are next in energy (Figure 8); immediately below the HOMO in energy is the d_{xy} orbital, followed by the d_{z^2} orbital, and finally the $d_{xz,yz}$ pair. Overall, in fungal laccase the splitting of the d manifold appears to increase relative to plastocyanin. In addition, the separation between d_{xy}, d_{yz}, and d_{xy} decreases, causing these transitions to be grouped close in energy. These observations are consistent with the experimentally observed trends in the transition energies of fungal laccase relative to plastocyanin.

The next four orbitals are formally charge transfer in nature, involving S_{Cys} π and pseudo-σ interactions, as well as π_1 type orbitals on each of the imidazole (Im) rings. Although they are in the experimentally observable energy region,[70] the Im π_1 orbitals are not expected to have significant CT intensity, since they have little overlap with the HOMO; the electron density in the π_1 orbitals is predominantly on nonligating atoms of the Im rings, which do not contribute to the HOMO. Below the Im π_1 orbitals in energy are the Im π_2 CT orbitals, which *do* have a significant contribution from the ligating N^{δ}(His). These are followed by the S_{Cys} σ interaction that mainly involves the S^{γ} and C^{β} of the thiolate.

In passing, we note that calculations using the 2.19 Å Cu−S_{Cys} from the crystal structure[9] give a covalent HOMO with only 26% thiolate character. This HOMO is similar in general appearance to that in Figure 7. However, the decreased covalency, relative to plastocyanin, for the calculation using the crystallographic 2.19 Å Cu−S distance is inconsistent with the experimentally observed increase in covalency and the strength of the Cu−S bond indicated by the resonance Raman spectra. The 2.067 Å bond length used in the calculations (Figure 8 and Table 4) is within the precision of the fungal laccase crystal structure at 1.9 Å resolution.

(70) Dong, S. L.; Spiro, T. G. *J. Am. Chem. Soc.* **1998**, *120*, 10434−10440.

Discussion

The major differences between the T1 Cu centers in the crystal structures of plastocyanin[10] and fungal laccase[9] are the presence of the axial ligand and the position of the Cu atom with respect to the $N_{His}-N_{His}-S_{Cys}$ plane. This study focuses on the effect that such geometric changes will have on the electronic structure of the T1 Cu site. Absorption, CD, MCD, EPR, and resonance Raman data demonstrate that the high-potential T1 Cu site in fungal laccase exhibits a number of significant electronic structure differences compared to the classic blue copper site in plastocyanin. The d → d bands move to higher energy, reflecting an increase in the strength of the ligand field. This shift in the ligand field causes the *g* values to decrease. The decreased *g* values in fungal laccase account for about 50% of the observed increase in the hyperfine coupling, with the remaining change coming from a decrease in 4s mixing. The increased oscillator strength and the previously published ENDOR results[58] suggest a 30% increase in S covalency in the fungal laccases. Similarly, resonance Raman data provide direct evidence that the Cu−S bond is stronger in the fungal laccases. These experimental results are supported by Xα-SW calculations, which predict an increase in the ligand field and an increase in covalency of the Cu−S_{Cys} bond upon going from the plastocyanin site to the fungal laccase T1 site.

Origin of the Changes in Electronic Structure. The origin of the experimentally observed changes in the electronic structure between the T1 site in plastocyanin and fungal laccase can be determined by using density functional calculations to evaluate hypothetical intermediate geometries. The main geometrical differences between plastocyanin and the T1 Cu site in fungal laccase involve elimination of the axial S_{Met} ligand at 2.82 Å, a 0.36 Å shift of the Cu atom into the N_2S plane, and small differences in the S−Cu−N angles. Figure 8 summarizes the electronic structure changes associated with a series of geometric perturbations that transform the plastocyanin structure into the fungal laccase structure. For all structures considered, the HOMO was similar in appearance to that in plastocyanin: highly covalent with a strong π-type antibonding interaction between the Cu $d_{x^2-y^2}$ orbital and the S_{Cys} p π orbital. In intermediate structure A, the axial Met of plastocyanin is removed while maintaining the remaining structure. This perturbation causes the covalency to increase from 35% in plastocyanin to 37%, as observed in the fungal laccase calculation. A series of ADF calculations in which the Cu−S_{Met} distance is progressively lengthened and then removed suggest that this increase in S_{Cys} donor character results from charge compensation for the lost axial S_{Met} ligand residue. Figure 8 (top) includes the results of these calculations on Δq(Cys) (the change in charge donation from the Cys). For intermediate structure A, the fully occupied levels of the d manifold shift to deeper energy relative to plastocyanin by an amount that is about half the shift observed in the fungal laccase calculation. Finally, intermediate A reproduces the experimentally observed grouping of the d_{xy}, d_{yz}, and d_{xz} transitions.

Intermediate structure B is created by shifting the Cu atom into the N_2S plane while maintaining ligand distances identical to those of plastocyanin and intermediate structure A. Here, the percent covalency (from Xα) and the amount of Cys charge donation estimated by ADF calculations are roughly the same as in A. However, moving the Cu atom into the N_2S plane shifts the d manifold to even deeper energy relative to the $d_{x^2-y^2}$ orbital,

consistent with the experimentally observed increase in LF transition energies in fungal laccase. This geometric perturbation also reproduces the experimentally observed grouping of the d_{xy}, d_{yz}, and d_{xz} transitions.

Finally, making small adjustments to the angular positions of the Cu ligating atoms (as in the fungal laccase structure) has little effect on either the covalency of the site or the relative energies of the d orbitals.[71] This series of calculations reveals that the key feature in the formation of the fungal laccase site is the removal of the axial ligand and concomitant increase in the S_{Cys} donor strength. Note that these distortions are coupled, since the absence of an axial ligand will result in a shift of the Cu atom into the $(N_{His})_2S_{Cys}$ plane.

Origin of the High Redox Potential. Numerous proposals have suggested that the high reduction potential typically observed in the fungal laccases results from the lack of the axial methionine ligand.[16,72,73] Such a geometry would stabilize the reduced site at the expense of the oxidized site because of the loss of a ligand donor interaction, albeit a weak one. This would cause the reduction potential to increase. No significant differences in the electronic structure of the T1 site in M.t. laccase, R.s. laccase, and P.p. laccase could be discerned even though the reduction potential of the T1 Cu in these enzymes differs by 300 mV (Table 1). This large range in potential suggests that, as is generally recognized, other factors such as solvent accessibility, the orientation of dipoles, and hydrogen bonding play an important role in tuning the $E°$ of this site.[74] However, this does not preclude the importance of the ligand environment in significantly contributing to the reduction potential. The $E°$ values of the T1 site in all three fungal laccases studied are substantially higher than typically observed for blue copper proteins. To evaluate the contribution of the ligand environment, it is instructive to systematically examine the impact of each ligand by site-directed mutagenesis within a fixed protein environment.

The F463M mutant of the high-potential P.p. laccase enables the role of the axial methionine to be evaluated while keeping the remaining protein environment constant. The absorption, CD, MCD, EPR, and resonance Raman data for the axial mutant all reveal a systematic perturbation to the T1 Cu electronic structure, consistent with the mutant site becoming more like the site in plastocyanin. From the electronic spectra and EPR parameters, the ligand field of the F463M mutant is between that of the wild-type enzyme and plastocyanin. The increase in the $\langle \nu_{Cu-S} \rangle$ value obtained from resonance Raman spectroscopy indicates that the strength of the $Cu-S_{Cys}$ bond decreases in F463M. Further, the covalency of the $Cu-S_{Cys}$ bond decreases, as reflected by the oscillator strength of the absorption spectrum. These results suggest that the methionine contribution to the electronic structure of the T1 site is beyond a simple change in the local dielectric caused by the Phe → Met mutation and is consistent with a weak bonding interaction. Importantly, upon changing the axial Phe to Met, the $E°$ decreases 100 mV, from 780 to 680 mV.[30] The extent of the change is consistent with reciprocal studies on *Pseudomonas aeruginosa* azurin in which the naturally occurring axial Met was mutated to a variety of other amino acids including those with noncoordinating groups such as Leu ($E°$ increased 102 mV) and Ile ($E°$ increased 128 mV).[75]

Ligand Field Trends with Axial Interaction. Given the experimental assignment of the ligand field transitions (see Appendix), correlations can be made between the energy of the z^2 transition and the strength of the interaction in the z direction (i.e., approximately along the Cu−axial ligand bond). Examination of *Alcalagenes denitrificans* azurin (A.d. Az) and its M121Q mutant reveals that the z^2 transition (band 8) decreases in energy when the stronger O^{ϵ}(Gln) ligand ($r_{Cu-O} = 2.26$ Å) replaces the weak S(Met) ($r_{Cu-S} = 3.11$ Å) in the axial position.[76] Thus, the energy of the z^2 transition decreases as the strength of the axial ligand increases, as would be expected considering d_{z^2} is antibonding with respect to the axial ligand. In P.p. laccase the energy of the z^2 (band 8) transition is remarkably high at ~6900 cm^{-1}, consistent with the complete absence of an axial ligand. In the P.p. laccase F463M mutant, the energy of band 8 decreases to 6500 cm^{-1}, indicating a stronger axial interaction than in laccase.

We also note that the splitting between the $x^2 - y^2$ and xy orbitals is related to the presence of a Jahn−Teller force that could occur in the oxidized blue copper site; the smaller the splitting, the more the site will be subject to distortion along the tetragonal coordinate described in ref 23 and also in refs 55 and 56. The geometry of the blue copper site in fungal laccase splits these orbitals sufficiently in energy such that structural reorganization upon oxidation is expected to be minimized, therefore allowing efficient electron transfer. It should also be recognized that the high covalency of the $Cu-S_{Cys}$ bond provides an efficient superexchange pathway for electron transfer from the T1 Cu to the T2/T3 Cu cluster.

Summary

We have provided a detailed description of the electronic structure of the nonaxially ligated T1 Cu site in fungal laccase. The primary differences between this site and that of the classic blue copper site in plastocyanin are the increased covalency of the $Cu-S_{Cys}$ bond and the increased strength of the ligand field. Both of these changes derive from removal of the axial ligand. Experimental studies on the F463M mutant of fungal laccase indicate that replacing the nonligating axial Phe with a weakly ligating axial Met significantly perturbs the structure of the T1 Cu, decreasing the covalancy of the $Cu-S_{Cys}$ bond, the ligand field strength, and the reduction potential (by 100 mV). In addition to the direct ligand environment, the protein matrix is also found to play a critical role in determining the reduction potential of the T1 Cu site. Our experimental results are supported by electronic structure calculations that show that removal of the axial ligand causes the $Cu-S_{Cys}$ to compensate for the reduced donor interaction. This study clearly establishes that the presence of the axial ligand impacts the electronic structure of the blue copper site.

Acknowledgment. We gratefully acknowledge Anders Pedersen and Gideon Davies for providing us with the crystal structure coordinates for *Coprinus cinereus* laccase and Dr. Frank Neese for extremely valuable discussions regarding MCD theory. This research was supported by NIH Grant DK31450

(71) Relative to intermediate structure B, the small shift in the energy of the *xy* orbital for the final fungal laccase model likely results from the small increase in the N−Cu−N angle, which places the Cu−N bonds slightly closer to the *xy* orbital, thereby increasing the antibonding interaction.

(72) Gray, H. B.; Malmström, B. G. *Comments Inorg. Chem.* **1983**, *2*, 203−209.

(73) Wittung-Stafshede, P.; Hill, M. G.; Gomez, E.; Di Bilio, A. J.; Karlsson, B. G.; Leckner, J.; Winkler, J. R.; Gray, H. B.; Malmström, B. G. *J. Biol. Inorg. Chem.* **1998**, *3*, 367−370.

(74) Stephens, P. J.; Jollie, D. R.; Warshel, A. *Chem. Rev.* **1996**, *96*, 2491−2513.

(75) Pascher, T.; Karlsson, B. G.; Nordling, M.; Malmström, B. G.; Vänngård, T. *Eur. J. Biochem.* **1993**, *212*, 289−296.

(76) Romero, A.; Hoitink, C. W. G.; Nar, H.; Huber, R.; Messerschmidt, A.; Canters, G. W. *J. Mol. Biol.* **1993**, *229*, 1007−1021.

(E.I.S.) and NSF Grant CHE 9528250 (E.I.S.). D.W.R. is supported by an N.I.H. postdoctoral fellowship GM 18812.

Appendix: Assignment of the Ligand Field Transitions

There continues to be a discrepancy between the ordering of two ligand field transitions predicted by electronic structure calculations[55,56,68,77] and the experimental spectral assignment of these transitions.[19,21,23,35] These differences may be due to poor descriptions for the Cu and S wave functions in such highly covalent centers. The two highest energy ligand field bands are shown by both experiment and calculations to be associated with the *xz* and *yz* transitions, which typically exhibit a pseudo-*A*-term MCD feature.[78] However, calculations of blue copper sites predict that the lowest energy band (8) should be the $xy \rightarrow x^2 - y^2$ transition and the next highest energy band (7) should be the $z^2 \rightarrow x^2 - y^2$ transition,[55,68,77] whereas experimental results indicate the opposite assignment.[23] The original assignment of the experimental ligand field bands in ref 19 attributed the low-energy transition (band 8) to $z^2 \rightarrow x^2 - y^2$ and the next transition (band 7) to $xy \rightarrow x^2 - y^2$ on the basis of analysis of MCD signs. Similarly, the method of calculating *C*-term MCD signs outlined in ref 60, which includes spin−orbit coupling with both the ground and excited state as well as the transition polarizations, reinforces this early assignment; for plastocyanin, the $z^2 \rightarrow x^2 - y^2$ transition is calculated to be positive and is thus assigned to band 8 while the $xy \rightarrow x^2 - y^2$ is calculated to be negative and is assigned to band 7. Further insight into this assignment can be obtained by examining the experimental transition energies of bands 7 and 8 over a series of blue Cu proteins (Table 5) along with the $g_{\|}$ value, which provides an independent estimate of the *xy* energy ($\Delta g_{\|} \propto 1/E_{xy}$; see eq 2). This feature of the ligand field assignment is important, since the $z^2 \rightarrow x^2 - y^2$ transition energy can provide an experimental probe of the strength of the axial ligand field.

The blue Cu site in *Achromobacter cycloclastes* nitrite reductase (Ac NiR) has a $g_{\|}$ value of 2.19, the classic blue Cu site in plastocyanin (PLC) has a $g_{\|}$ value of 2.226, and *Rhus vernicifera* stellacyanin (Rv Stc) has a $g_{\|}$ value of 2.287. Relative to PLC (5000 cm^{-1}), band 8 is at higher energy in both Ac NiR (5600 cm^{-1}) and Rv Stc (5500 cm^{-1}), but the differences are small. The large difference in the $g_{\|}$ values of Rv Stc and Ac NiR is therefore difficult to rationalize if band 8 is attributed to d_{xy}. Alternatively, band 7 in PLC (10 800 cm^{-1}) is at an energy between that of Rv Stc (8750 cm^{-1}) and Ac NiR (11 900 cm^{-1}), and therefore, when band 7 is assigned as the $d_{xy} \rightarrow d_{x^2-y^2}$ transition, the trend in $g_{\|}$ is a straightforward reflection of the different ligand fields associated with the different sites. Similarly, in cucumber basic protein (CBP, $g_{\|} = 2.207$), band 8 is slightly higher in energy (5800 cm^{-1}) than in Ac NiR (5600 cm^{-1}), yet the $g_{\|}$ value of the former is larger. Conversely, band 7 in CBP (10 800 cm^{-1}) is at lower energy than in Ac NiR (11 900 cm^{-1}), and therefore, the change in $g_{\|}$ is again consistent with assigning this transition to d_{xy}. To minimize the influence of differences in protein structure on the transition energies and *g* values, the wild type *Alcalagenes denitrificans* azurin (A.d. Az) can be compared with a point mutant, M121Q, where the axial Met ligand has been replaced with a Gln. Both bands 7 and 8 decrease in energy (Table 5) upon mutation; the larger magnitude (~2000 cm^{-1}) of the decrease in band 7 compared to band 8 (~300 cm^{-1}) is again consistent with the radical change in $g_{\|}$ from 2.255 in A.d. Az to 2.29 in M121Q. On the basis of these considerations, it seems clear that band 7 can be experimentally assigned to the $d_{xy} \rightarrow d_{x^2-y^2}$ transition, while band 8 can be assigned to the $d_{z^2} \rightarrow d_{x^2-y^2}$ transition.

Table 5. Spectral Summary d → d Bands of Blue Copper Proteins[a]

band		Ac NiR[b]	Rv STC[c]	PLC[b]	CBP[c]	Ad Az[c]	Ad Az M121Q[c]	P.p. laccase
8	z^2	5600	5500	5000	5800	5800	5500	6900
7	*xy*	11900	8750	10800	10800	10800	8750	13300
6	*yz*	13500	11200	12800	12900	12800	11200	14350
5	*xz*	14900	12800	13950	14100	13950	12800	15850
g_z		2.19	2.287	2.226	2.207	2.255	2.287	2.194

[a] Band positions are given in cm^{-1}. [b] From ref 23. [c] From ref 21.

Supporting Information Available: Absorption and CD spectra of the F^- derivative of P.p. laccase before and after the addition of ascorbate, Abs, CD, and MCD spectra of M.t. and R.s. laccase, tables of the Cartesian coordinates used in SCF-Xα calculations (PDF). This material is available free of charge via the Internet at http://pubs.acs.org.

JA991087V

(77) Neese, F. Personal communication.

(78) As discussed above, this feature is distorted in the fungal laccases because of spectral overlap of the tightly grouped ligand field bands.

(79) Gordy, W. In *Theory and Applications of Electron Spin Resonance*; Gordy, W., Ed.; John Wiley and Sons: New York, 1980.